Graphite-Polyurethane and Graphite-Silicone Rubber Composite Electrodes for Electrochemical Characterization and Determination of Minoxidil

Rogerio A. Sousa,[a, c, d] *Sidney X. Dos-Santos*,[b] *Eder T. G. Cavalheiro*,[b] *Christopher M. A. Brett**[c]

[a] Departamento de Química, Universidade Federal de São Carlos, 13.565-905, São Carlos, SP, Brazil
[b] Instituto de Química de São Carlos, Universidade de São Paulo, 13.560-970, São Carlos, SP, Brazil
[c] Departamento de Química, Faculdade de Ciências e Tecnologia, Universidade de Coimbra, 3004-535 Coimbra, Portugal
tel: 351-239-854470; fax: +351-239-827703
[d] Current address: Centro Universitário das Faculdades Associadas (UNIFAE), Largo Eng. Paulo de Almeida Sandeville, 15, 13870-377, São João da Boa Vista, SP, Brazil
*e-mail: brett@ci.uc.pt

Received: November 7, 2012
Accepted: January 9, 2013
Published online: February 22, 2013

Abstract
Graphite-polyurethane (GPUE) and graphite-silicone rubber (GSRE) electrodes have been used for oxidative determination of the vasodilator minoxidil in pharmaceutical samples and in plasma and urine electrolyte solutions. The electrooxidation process at 0.840 V (GPUE) and 0.860 V (GSRE) vs. SCE was characterized over a wide pH range by cyclic voltammetry and electrochemical impedance spectroscopy. Quantification using cyclic, differential pulse, and square-wave voltammetry, gave results agreeing with high pressure liquid chromatography, that has similar micromolar detection limits, but with a simpler analytical procedure. Advantages of these composite electrodes are non-adsorption of analyte or oxidation products, a long useful life and robustness.

Keywords: Composite electrode, Graphite-polyurethane electrode, Graphite-silicone rubber electrode, Minoxidil

DOI: 10.1002/elan.201200606

1 Introduction

Minoxidil (2,4-diamino-6-piperidinopyrimidine-3-oxide, MX, Scheme 1) is an odorless white crystalline powder, insoluble in water, acetone or alkaline solutions, slightly soluble in alcohols, and freely soluble in acidic solutions [1], with $pK_a = 4.6$ [2]. MX has been used as an orally administrated peripheral vasodilator drug, applied in the treatment of refractory hypertension patients [3]. Excessive oral administration of this drug causes liquid retention and hirsutism [4]. Initially described as an antihypertensive drug, MX has also had new applications in dermatology, especially in the treatment of androgenic alopecia [4,5]. In this case, this drug has been topically applied in order to stimulate hair growth by inducing vasodilation with consequent increase in the local irrigation and blood flow [5]. Commercially available topical use formulations typically contain 2% MX (20 mg mL^{-1}), in ethanol/propyleneglycol or their mixture with 2-*n*-nonyl-1,3-dioxolane as a vehicle [6,7].

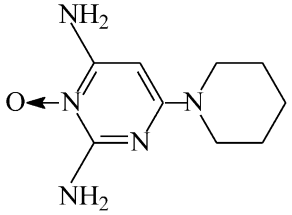

Scheme 1. Structural formula of MX.

The literature describes MX determination using liquid chromatography [8,9], photometric titrations [10], UV-vis spectrophotometry [11] and flow injection with both photometric [4,12] and amperometric [13] detection procedures. Electroanalytical procedures based on reduction using differential pulse polarography [3] and polarography plus spectrophotometry [14] have been reported.

The use of composite electrodes, which are defined by Tallman and Petersen [15] as *"a material consisting of at least one conducting phase commingled with at least one insulating phase"*, as detectors in electrochemical analysis is becoming common. In such materials the insulator phase acts as an agglutinant. These electrodes can be classified according to the way in which the conductor and the insulator are distributed within the material. In particular, disperse composite materials in which graphite is agglutinated by polymers present good properties for use as electrochemical sensors [16–19].

The purpose of this work is to investigate the voltammetric behaviour of MX using composite electrodes

based on graphite/polyurethane resin (GPUE) 60% (graphite, *m/m*) and on graphite/silicone rubber (GSRE) 70% (graphite, *m/m*). The possibility of quantitatively determining MX at such electrodes also was investigated. These GPUE [16] and GSRE [20,21] composites have been shown to be useful in cyclic voltammetry (CV), differential pulse voltammetry (DPV) and square wave voltammetry (SWV) determination of different analytes, including in flow analysis with amperometric detection.

Examples of applications involving these composite electrodes are the determination of verapamil and its release profile from commercial tablets [22], the determination of atenolol [23] and paracetamol [24] using flow injection analysis (FIA) with amperometric detection, paracetamol at a molecularly imprinted polymer modified GPUE [25] and furosemide [26], rutin [27] and dopamine in synthetic cerebrospinal fluid [28] by DPV.

Application of GPUE and GSRE composite electrodes to the determination of MX in pharmaceutical formulations, based on the electrooxidation of the analyte, is described. The accuracy of the proposed electrochemical determination was compared with results from a high performance liquid chromatography (HPLC) procedure described by Zarghi et al. [8] and showed good agreement.

2 Experimental

2.1 Reagents and Solutions

All reagents were of analytical grade and used as received. Solutions were prepared using water purified in a Millipore Milli-Q system (resistivity $>18\,M\Omega\,cm$). A $1.0\times10^{-2}\,mol\,L^{-1}$. MX stock solution was prepared daily in ethanol/water 1:1 (v/v) mixture.

Supporting electrolyte solutions (pH 2.0 to 8.0) were prepared in order to evaluate the electro-oxidation of MX at different pH values and to search for the best analytical conditions, see Table 1.

2.2 Graphite Polyurethane Composite Electrode Preparation

As previously described [16], the GPUE was prepared with a vegetable oil derivative polyurethane resin by mixing 1.0 part of hardener A-249 and 0.85 parts of polyol B-471 (Poliquil, Brazil), according to the manufacturer's instructions. Appropriate amounts of graphite powder, 1–2 μm (Aldrich, USA) were added to the polymer in order to obtain a composite containing 60% graphite (*m/m*), which is the composition that presented the best electroanalytical response according to Mendes et al. [16]. This mixture was homogenized in a glass mortar during 15 min and then extruded as 3.0 mm diameter rods. The rods were let to cure for 24 h at around 25 °C and then cut into 1 cm sections.

Table 1. Electrolyte solutions.

Component A [a,b]	Component B [a,b]	pH
6.5 mL HCl	25.0 mL KCl	1.97
3.20mL HCl	25.0 mL KCl	2.55
46.3 mL HOAc	3.7 mL NaOAc	3.17
36.8 mL HOAc	13.2 mL NaOAc	3.88
8.80 mL HOAc	41.2 mL NaOAc	4.96
43.9 mL NaH_2PO_4	6.15 mL Na_2HPO_4	5.91
19.5 mL NaH_2PO_4	30.5 mL Na_2HPO_4	7.01
2.65 mL NaH_2PO_4	42.4 mL Na_2HPO_4	7.94

[a] Component concentrations 0.20 M; [b] Components A and B are mixed and water added to 100 mL.

Electrical contacts were made by attaching the composite rods to copper wire with the help of a silver epoxy (EPO-TEK 410E, Epoxy Technology, USA). This assembly was inserted into a glass tube ($\varnothing_i=0.5$ cm, $l=7.0$ cm) and sealed with nonconducting epoxy resin (SQ 2004 – Silaex, Brazil). The surfaces were polished using abrasive paper followed by 1.0 μm α-Al_2O_3 in a polishing wheel (Arotec, Brazil). After that the electrodes were sonicated in 2-propanol and water during 5 min in each solvent.

2.3 Graphite Silicone Rubber Composite Electrode Preparation

The GSRE was prepared with commercial silicone rubber (SR) and graphite powder, 1–2 μm (Aldrich, USA) in the ratios 70% graphite and 30% SR (*m/m*), described by Oliveira et al. [21] as the composition that presents the best analytical response. This mixture was homogenized in a glass mortar during 15 min and then encapsulated in a glass tube of 3.0 mm internal diameter. The assembly was pressed at 0.5 atm with a copper rod ($\varnothing=3.0$ mm) for 24 h, at around 25 °C, to cure the SR adhesive.

Contacts were made using silver epoxy (EPO-TEK 410E, Epoxy Technology, USA) and copper wire. The electrode surface was polished using abrasive paper followed by 1.0 μm α-Al_2O_3 on a polishing wheel (Arotec, Brazil). After that the electrodes were sonicated in 2-propanol and in water during 5 min in each solvent.

2.4 Instruments

Voltammetric experiments were carried out with a computer-controlled μ-Autolab Type II potentiostat/galvanostat controlled by GPES 4.9 software (Metrohm-Autolab, Netherlands). A three electrode cell, with 20 mL full capacity, was used in a three electrode configuration; the reference electrode was a saturated calomel electrode (SCE) and the counter electrode was platinum foil (area 1 cm^2) and the composites were the working electrodes.

Electrochemical impedance measurements were carried out in the same electrochemical cell with a PC-controlled Solartron 1250 Frequency Response Analyser coupled to a Solartron 1286 Electrochemical Interface using ZPlot 2.4 software (Solartron Analytical, UK). Frequency scans were done from 65 000 Hz down to 0.1 Hz with ten measurements per frequency decade, using a sinusoidal voltage perturbation of 10 mV rms.

2.5 Commercial Samples

The commercial Regaine (Pharmacia, USA), Loniten (Rhodia Pharma, Brazil) and a Magistral formulation (Porto Bianco, Brazil), were used as samples in this work. The Regaine and Magistral formulations were presented in liquid form for topical use, containing 2% (20 mg mL^{-1}) MX and 5% (50 mg mL^{-1}) MX respectively; in both formulations the vehicle was a mixture of ethanol and propylene glycol. A stock solution of 1.0×10^{-3} mol L^{-1} of MX solution was prepared by adding the appropriate amount of sample to 1:1 H_2O/ethanol (v/v) in a 50 mL volumetric flask, from which an appropriate aliquot was diluted in the supporting electrolyte pH 2 for analysis.

Loniten is supplied in tablets labeled as containing 10 mg of MX and the excipients lactose, microcrystalline cellulose, starch, colloidal silicon dioxide and magnesium stearate. Samples were prepared by grinding 10 tablets in a glass mortar. After careful homogenization, a mass equivalent to that of one tablet was accurately weighed (±0.1 mg) and the MX extracted with ethanol. An aliquot of this ethanol solution was diluted in 1:1 H_2O/ethanol solution (v/v) in order to be 5.0×10^{-4} mol L^{-1} in MX, from which an appropriate aliquot was diluted in the supporting electrolyte pH 2 for analysis.

2.6 Application in Synthetic Plasma and Urine Electrolyte Solutions

The electroanalytical procedures proposed in this paper were also used for the quantification of MX contained in synthetic plasma [29] and urine [30] electrolyte solutions. An exact mass of MX was dissolved in exact volumes of synthetic plasma and urine electrolyte solutions, in order to reach a final concentration of 25.0×10^{-6} mol L^{-1}, from which an appropriate aliquot was diluted in the supporting electrolyte pH 2 for analysis. The compositions of the synthetic plasma and urine electrolyte solutions are presented in Table 2.

Table 2. Composition of the synthetic plasma and urine electrolyte solutions [29,30].

Components	Quantity of constituents (g L^{-1})	
	Urine	Plasma
$CaCl_2{\cdot}2H_2O$	1.103	–
NaCl	2.925	8.036
Na_2SO_4	2.25	0.072
KH_2PO_4	1.40	–
KCl	1.60	–
NH_4Cl	1.00	–
$NaHCO_3$	–	0.352
KCl	–	0.225
$Na_2HPO_4{\cdot}3H_2O$	–	0.238
$MgCl_2{\cdot}6H_2O$	–	0.311
$CaCl_2$	–	0.293
pH	6.0	7.4

2.7 Comparison Method

In order to investigate the accuracy of the proposed electroanalytical procedures the results were compared with those from a chromatographic method described by Zarghi et al. [8].

In such experiments the commercial samples, treated exactly as described above, were analyzed by HPLC under the experimental conditions: mobile phase 80:20 (v/v) methanol/water, 1.3 mL min^{-1} flow rate, UV detection at 254 nm, C-18 (150×3.9 mm) Supelco column, in a liquid chromatographic system HPLC LC-6AD equipped with a spectrophotometric detector SPD-10A VP, both from Shimadzu, Japan.

3 Results and Discussion

3.1 Electroactive Area of Composite Electrodes and Diffusion Coefficient of MX

The electroactive surface areas of both composite electrodes were determined by cyclic voltammetry, using 5.0×10^{-3} mol L^{-1} potassium hexacyanoferrate(II) in 0.50 mol L^{-1} KCl solutions at different potential scan rates (10–100 mV s^{-1}), by means of the Randles–Sevcik Equation (Equation 1) [31]:

$$I_{p,a} = 2.69\times10^{5} n^{3/2} A D_R{}^{1/2} C v^{1/2} \quad (1)$$

in which n is number of electrons involved in the oxidation, A is the electroactive area (cm^2), D_R is the diffusion coefficient of hexacyanoferrate(II), taken as 7.7×10^{-6} cm^2 s^{-1} in 0.50 mol L^{-1} KCl [32], C is the bulk concentration of hexacyanoferrate(II) in mol cm^{-3}, and v the potential scan rate, in V s^{-1}.

From plots of peak current vs. scan rate the electroactive areas were found to be 0.093±0.002 cm^2, corresponding to 131% of the geometric area of the GPUE and 0.090±0.004 cm^2, corresponding to 127% of the geometric area of the GSRE. The larger electroactive than geometric area is attributed to the roughness of the composite surface [16].

Figure 1 shows a typical cyclic voltammetry profile in pH 2.5 electrolyte solution, where MX is in the protonated form, at different scan rates, the oxidation of MX being seen to occur at 0.84 V (vs. SCE). Plots of peak current vs. square root of scan rate were found to be linear ($I_{p,a}=0.0187v^{1/2}+0.667$; ($R=0.998$); $n=7$). Since MX oxidation is an irreversible process, the diffusion coefficient of MX was determined using Equations 2 and 3 [31]:

$$I_{p,a} = 2.99\times10^{5}\ n(\alpha_a n)^{1/2} A C_{MX} D_{MX}{}^{1/2} v^{1/2} \quad (2)$$

$$[E_p - E_{p/2}] = 47.7(\alpha_a n) \quad (3)$$

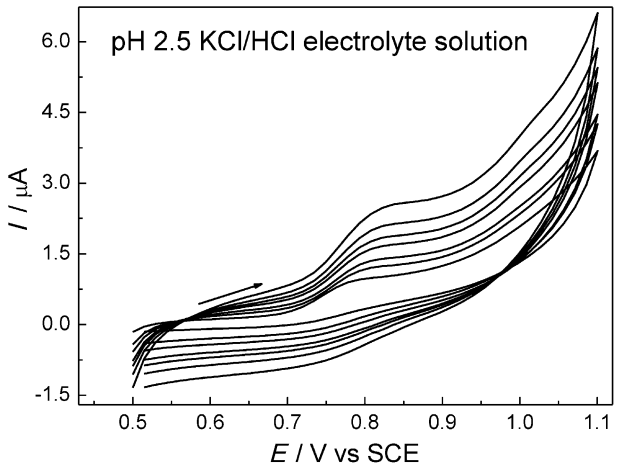

Fig. 1. Cyclic voltammogram of MX (6.25×10^{-4} mol L^{-1}) in pH 2.5 electrolyte solution at GPUE, scan rates 10–100 mV s^{-1}.

where α_a is the anodic charge transfer coefficient and n the number of electrons transferred. Application of Equation 3 gives $(\alpha_a n)=1.26$ and, from a plot of peak current vs. square root of scan rate, the diffusion coefficient of MX was found to be 8.0×10^{-6} cm^2 s^{-1} for both composites.

3.2 Electrochemical Impedance Spectroscopy

Electrochemical impedance spectroscopy (EIS) studies were performed in order to investigate the electrode process. The impedance spectra are shown in Figure 2 for both GPUE and GSRE composite electrodes and were recorded at the peak potential (~0.85 V vs. SCE) and at potentials lower and higher than the peak potential (+0.50 and +1.10 V vs. SCE), in both blank and 6.25×10^{-4} mol L^{-1} MX solutions, at pH 2.5 (GPUE) and 2.0 (GSRE).

An equivalent electrical circuit with a cell resistance, R_Ω, in series with a parallel combination of a constant phase element, *CPE*, and a charge transfer resistance is needed to fit the curves, in the case of GSRE a finite diffusion Warburg element also being needed. This is similar to what has been found with spectra at other composite electrodes [33]. In all cases, the *CPE*, $CPE=\{(C\ i\omega)^\alpha\}^{-1}$ models a non-ideal capacitor. The CPE was found to be necessary because of the heterogeneous nature of the electrode surface, expressed through the exponent α, with values that varied between 0.70 and 0.85.

Figures 2A1–2A3 present complex plane impedance spectra using the GPUE. Figure 2A1 shows spectra characteristic of a capacitance at a slightly rough surface without any charge transfer both in the presence and absence of MX in solution. The spectrum presented in Figure 2A2 was recorded at the oxidation peak potential of MX. In this spectrum, there is a large change in impedance compared to the curves of the blank with the curves of MX, similar to that at 0.50 V, showing the occurrence of charge transfer due to oxidation of MX. Finally, Figure 2A3 shows spectra exhibiting curvature in the absence of MX and reduction in the impedance values in relation to lower potentials. This can be attributed to oxidation of graphite and a small amount of evolution of oxygen, which also influences the spectrum in the presence of MX.

Figures 2B present impedance spectra recorded using the GSRE. Figure 2B2 shows the impedance spectrum of the peak potential for oxidation of MX (+0.86 V), the spectra in Figures 2B1 and 2B3 are recorded at +0.50 and +1.10 V respectively. The impedance magnitudes are all smaller than at GPUE by a factor of 3 to 4. Additionally, there is more evidence of charge transfer processes at all the potentials tested than with GPUE, which shows the importance of the insulating matrix of the composite electrode. It suggests that the GSRE is not as inert as the GPUE and evidence of reactions of the electrode itself are seen at all three potentials.

In other experiments, impedance spectra were recorded before and after performing 15 voltammetric cycles in both blank and 6.62×10^{-4} mol L^{-1} MX solutions, at pH 2.5 (GPUE) and 2.0 (GSRE). In all cases the spectra were exactly the same, revealing that no irreversible adsorption takes place on the electrode surfaces.

3.3 Influence of pH and Mechanism of Oxidation

The influence of pH on the cyclic voltammetric response of MX was investigated in the range pH 2.0–8.0 (GPUE) and pH 2.0–7.0 (GSRE) in the +0.30 to +1.10 V (vs. SCE) potential interval at 25 mV s^{-1} scan rate, using a 6.25×10^{-4} mol L^{-1} MX solution. The results are presented in Figure 3, from which it is seen that the CV profiles are strongly dependent on the pH at both electrodes.

At the GPUE electrode, similar CV profiles can be observed (Figure 3A); however, the peak definition is not as good as at GSRE (Figure 3B). At GPUE in pH 2.5 solution a single peak was observed at +0.84 V (vs. SCE). When the pH is increased, this peak is shifted to lower potentials and a broader peak shape is observed. A second peak (not well resolved) appears from pH 5.2 at around +1.00 V.

At GSRE composites, pH 2.0, only one oxidation peak at 0.86 V vs. SCE can be observed (Figure 3B). This peak is shifted to lower potentials as the pH is increased, remaining practically constant from pH 4.6 (curve not shown) at around 0.68 V vs. SCE. When the pH reaches a value of 4.0 a second peak appears at +1.00 V and shifts to lower potential values as the pH increases.

Both the electrochemical reduction and oxidation mechanisms of MX are described in the literature. Amankwa et al. [3] proposed a mechanism for the reduction of MX, in which the N-oxide group is protonated and then converted to a secondary amine in a process involving one proton and two electrons and releasing water, at a carbon paste electrode. However, such processes are only seen in acidic medium, since at higher pH values the concentration of protonated N-oxide is negligi-

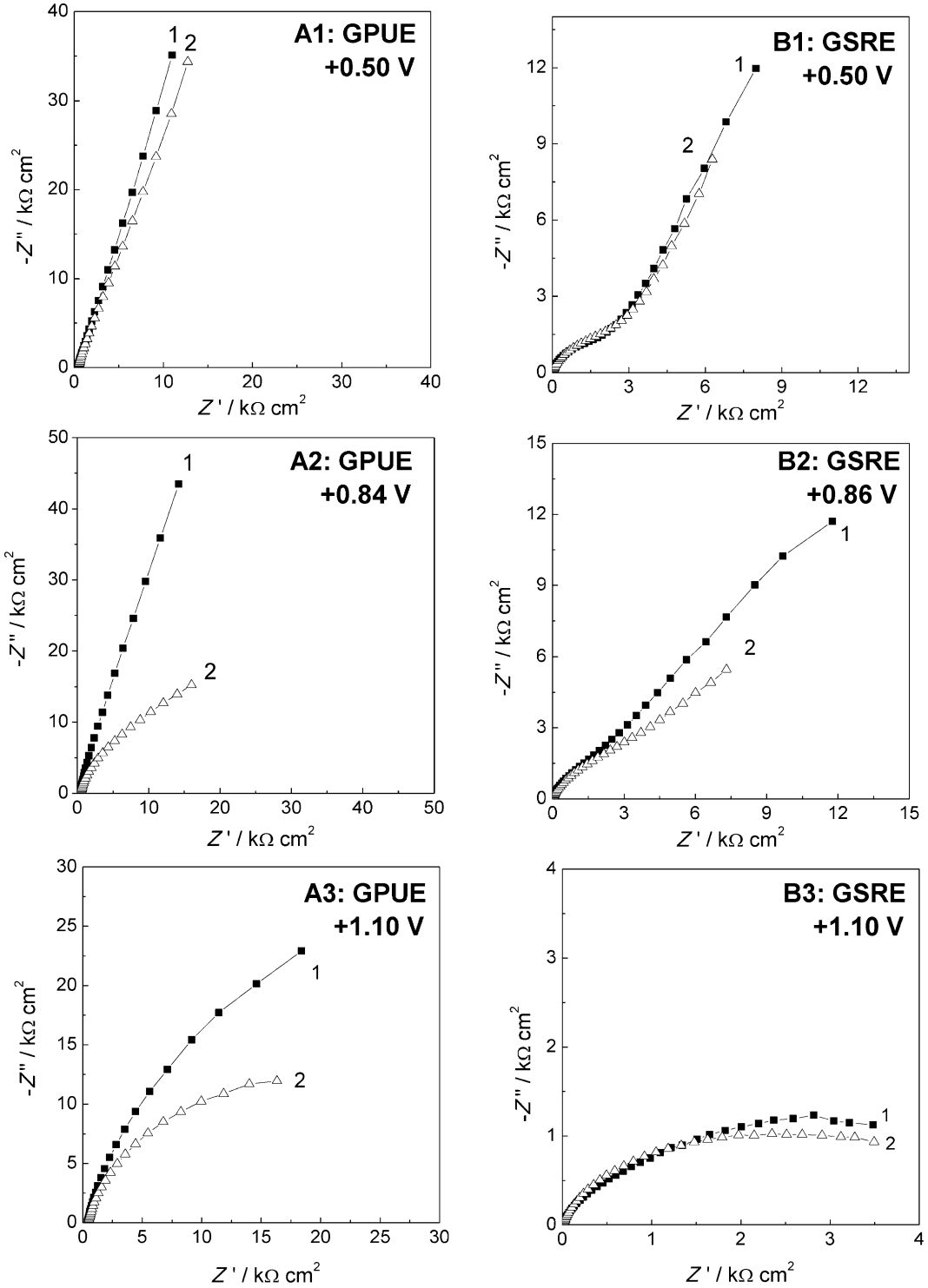

Fig. 2. Complex plane electrochemical impedance spectra at (A) GPUE and (B) GSRE at the indicated potentials; 1) blank, 2) $[MX] = 6.25 \times 10^{-4}$ mol L^{-1}.

ble and no reduction can occur. The reduction of MX was not used for quantitative purposes. In addition, the authors do not comment about the oxidative process in detail.

On the other hand, the electrooxidation mechanism of MX is still not totally clear in the literature. Chiang et al. [2] found $pK_a = 4.61$ for this compound, which was confirmed by Arcos et al. [14]. This pH is coincident with the appearance of the second oxidation peak as well as with the change in the slope of the E_p (first oxidation processes) vs. pH curve at both electrodes, see Figure 4, whose slopes were close to 65 mV for both electrodes. The value

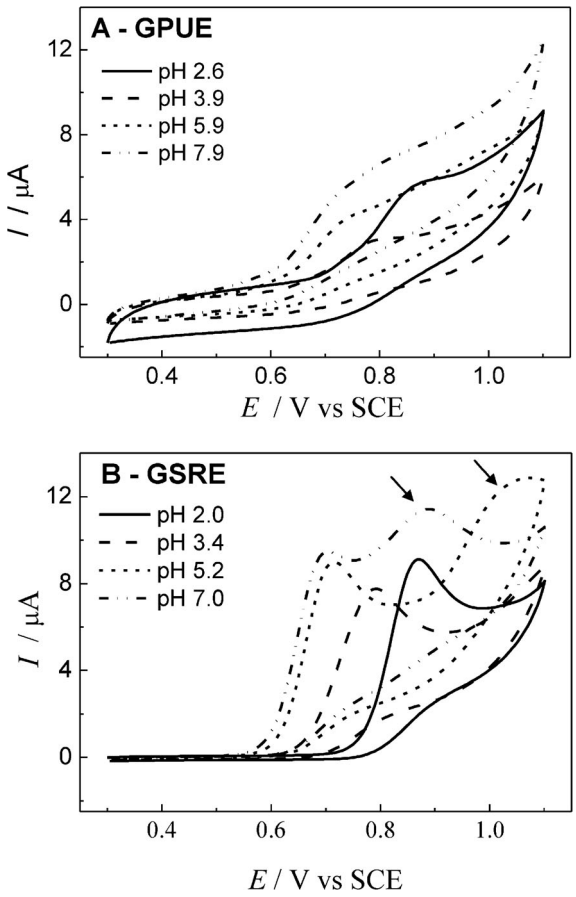

Fig. 3. Cyclic voltammograms of MX (6.25×10^{-4} mol L^{-1}) for different values of pH at A) GPUE; B) GSRE.

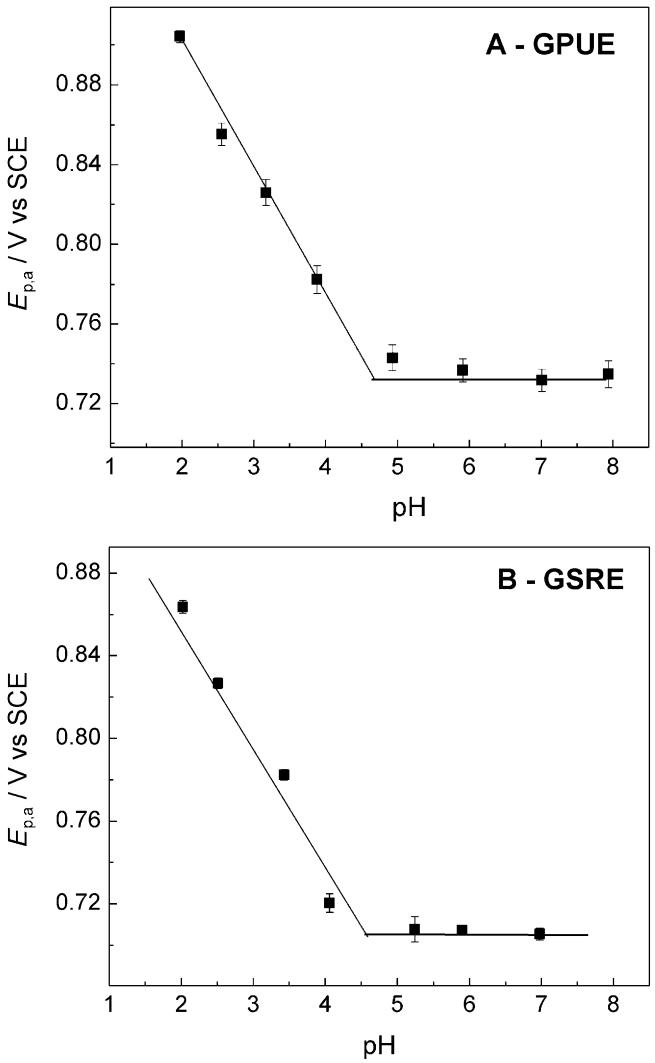

Fig. 4. Plots of peak potential, E_p, vs. pH for the first oxidation peak of MX (6.25×10^{-4} mol L^{-1}) from cyclic voltammograms ($v=25$ mV s^{-1}) at A) GPUE B) GSRE. The inclined lines have a slope of −59 mV per pH unit.

of the slope of the linear branches of the E_p vs. pH curves indicate that the same number of protons and electrons are involved in the first oxidation step. This may suggest that oxidation takes place when the primary amine group in the MX structure is protonated. After oxidation of the first amine group, it seems that the second one starts to oxidize, as a second peak appears, but only at higher pH. Oxidation in the amine groups has already been proposed by Pfaffen and Ortiz [13], comparing the potentials of MX oxidation at glassy carbon with those of different anilines. However, those authors did not investigate the acidic pH range, in which a single oxidation peak appears with good potential for use in quantitative determinations.

The best definition of signals at GPUE and GSRE was observed in KCl/HCl pH 2.5 solutions, with the oxidation peak at +0.840 V (vs. SCE, Figure 3A) and at pH 2.0, in which the oxidation peak was observed at +0.860 V (vs. SCE, Figure 3B), in both cases as an irreversible process.

In order to better understand the oxidation process, two CVs were recorded, using different initial sweep directions, at the GSRE electrode in pH 7.0 solution, since better resolution was observed than with GPUE (Figure 5). It is seen that the two processes are irreversible, only the oxidative branch of the CV appearing and that the second appears even when the sweep is started at potentials positive of E_p of the first process as in scan B.

The scans starting at different potentials suggest that the processes are independent, reinforcing the hypothesis of oxidation at different sites in the molecule, as stated above. Mathematical deconvolution of these overlapping peaks revealed that they strongly influence each other. Thus a highly acidic medium was chosen for further studies in order to prevent such interference, since in such conditions only the first peak is present.

3.4 Voltammetric Techniques for Determination of MX

3.4.1 Cyclic Voltammetry (CV)

A quantitative procedure was developed using cyclic voltammetry at GPUE, using as optimized parameters pH 2.5, scan rate of 25 mV s^{-1}, potential interval +0.50 to

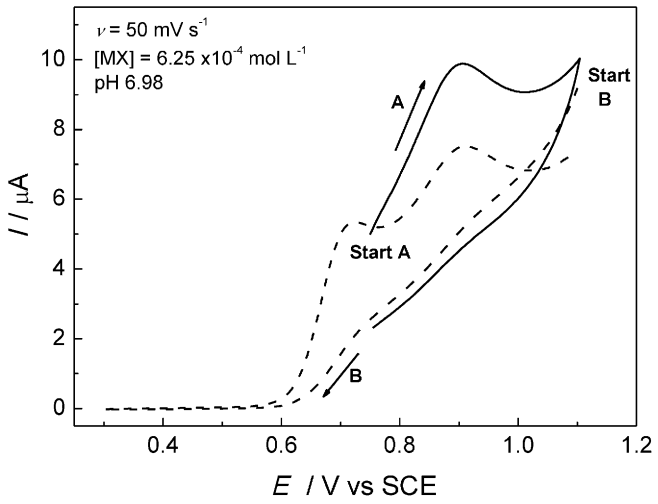

Fig. 5. Cyclic voltammograms at GSRE, pH 6.98: a) potential range +0.75 to +1.10 V vs. SCE starting in the positive direction, B) potential range +1.10 to +0.30 V vs. SCE starting in the negative direction. Scan rate 50 mV s^{-1}.

+1.10 V vs. SCE, and measuring the peak current in the first cycle. Under such conditions a linear dependence of peak current with MX concentration was observed, between 3.38×10^{-5} to 2.89×10^{-4} mol L^{-1}; ($I_{p,a}=0.53+5.76\times10^{4}$ C; $R=0.999_4$; $n=7$; where C is the concentration of MX in mol L^{-1}) and the limits of detection (LOD) and quantification (LOQ) [34] were 1.49×10^{-5} and 4.95×10^{-5} mol L^{-1}, respectively. When analyzing the commercial samples within the linear range of response, recoveries between 96 and 110 % at GPUE were observed.

MX was also quantified at the GSRE electrode under the following optimized conditions: pH 2.0; 50 mV s^{-1} scan rate; potential window +0.50 to +1.10 V vs. SCE, again measuring the peak current during the first cycle. These studies led to a linear dependence of peak current with MX concentration between 3.39×10^{-5} and 2.89×10^{-4} mol L^{-1}; ($I_{p,a}=0.29+5.24\times10^{4}$ C; $R=0.999_7$; $n=7$; where C is the analytical concentration of MX in mol L^{-1}) and the LOD and LOQ were 2.23×10^{-5} and 3.18×10^{-5} mol L^{-1}, respectively. Recovery assays led to values between 94 and 110 %.

Table 3 gives the concentration values obtained during application of the proposed method to analysis of commercial samples, together with the labeled and the chromatographic values. According to the *t*-Student test, the results from the proposed electrodes agree with those from the chromatographic procedure within a 90 % confidence level.

3.4.2 Differential Pulse Voltammetry (DPV)

For differential pulse voltammetry quantification, various parameters were optimized. First, a scan rate of 10 mV s^{-1} was fixed while amplitude modulations of 10, 25, 50, and 100 mV were tested and 100 mV was chosen. The scan rate was then optimized using 10, 25, 50, and 100 mV s^{-1} using 100 mV amplitude, and 50 mV s^{-1} was selected. The pH was taken as 2.5 for GPUE and 2.0 for GSRE, according to the data from cyclic voltammetry experiments; a +0.50 to +1.10 V (vs. SCE) potential window and 6.25×10^{-4} mol L^{-1} MX solutions were used. The DPV profiles obtained at both electrodes can be observed in Figures 6A and 6B.

The peak half-width, $W_{1/2}$, was ~95 mV for both electrodes, suggesting a one-electron irreversible process, in agreement with the results found by cyclic voltammetry [31].

DPV voltammograms of MX in different concentrations at a GPUE (Figure 6A) in pH 2.5 solution, revealed a peak at 0.72 V vs. SCE. The linear range was from

Table 3. Results of MX determination using voltammetric techniques (CV, DPV and SWV) at both GPUE and GSRE electrodes in comparison with the label and HPLC method.

Sample	Label	HPLC	CV			DPV			SWV		
			Found [a]	E_1 [b] (%)	E_2 [c] (%)	Found [a]	E_1 [b] (%)	E_2 [c] (%)	Found [a]	E_1 [b] (%)	E_2 [c] (%)
GPUE											
Regaine [d]	20	21.1±0.8	21.1±0.2	5.5	0	21.1±0.1	5.5	0	18.7±0.1	−6.5	−11.4
Loniten [e]	10	10.1±0.3	9.4±0.8	−6.0	−6.9	10.7±0.3	7.0	5.9	9.1±0.7	−9.0	−9.9
Magistral [d]	50	52.7±0.1	51±1	2.0	−3.2	52.4±0.1	4.8	−0.6	48±3	−4.0	−8.9
Urine [f]	25	–	23.80±0.06	−4.8	–	23.5±0.1	−6.0	–	25.1±0.2	0.4	–
Plasma [f]	25	–	22.62±0.08	−9.5	–	27.4±0.2	9.6	–	26.9±0.1	7.6	–
GSRE											
Regaine [d]	20	21.1±0.8	19.8±0.3	−1.0	−6.2	19.9±0.1	−0.5	−5.7	20.05±0.06	0.25	−4.9
Loniten [e]	10	10.1±0.3	10.6±0.7	6.0	4.9	9.5±0.3	−5.0	−5.9	10.3±0.3	3.0	1.9
Magistral [d]	50	52.7±0.1	52±5	4.0	−1.3	51.5±0.4	3.0	−2.3	46.1±0.2	−7.8	−12.5
Urine [f]	25	–	24±4	−4.0	–	25.90±0.03	3.6	–	26±1	4.0	–
Plasma [f]	25	–	27±4	8.0	–	26.4±0.8	5.6	–	26.8±0.3	7.2	–

[a] $n=3$, found±standard deviation; [b] relative error: $E_1=$[(found−label)/label]×100; [c] relative error: $E_2=$[(found−HPLC)/HPLC]×100; [d] mg mL^{-1}; [e] mg tablet^{-1}; [f] ×10^{-6} mol L^{-1}

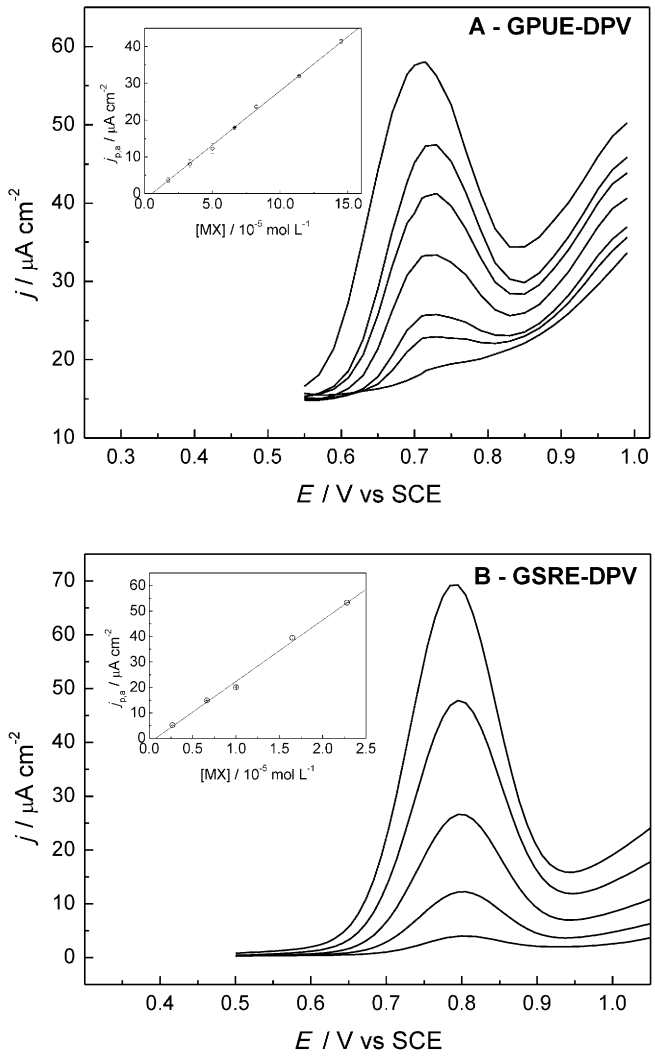

Fig. 6. Differential pulse voltammograms for oxidation of MX with different concentrations of MX. DP amplitude 100 mV, potential step 20 mV, interval between pulses 0.4 s. The insets show analytical curves. A) GPUE in HCl/KCl pH 2.5; [MX] = 1.75, 3.35, 5.02, 6.63, 8.24, 11.4 and 14.5×10^{-5} mol L^{-1}. $E_{p,a}$ = 0.720 V vs. SCE. B) GSRE in HCl/KCl pH 2.0; [MX] = 0.266, 0.664, 1.00, 1.65 and 2.28×10^{-5} mol L^{-1}. $E_{p,a}$ = 0.795 V vs. SCE.

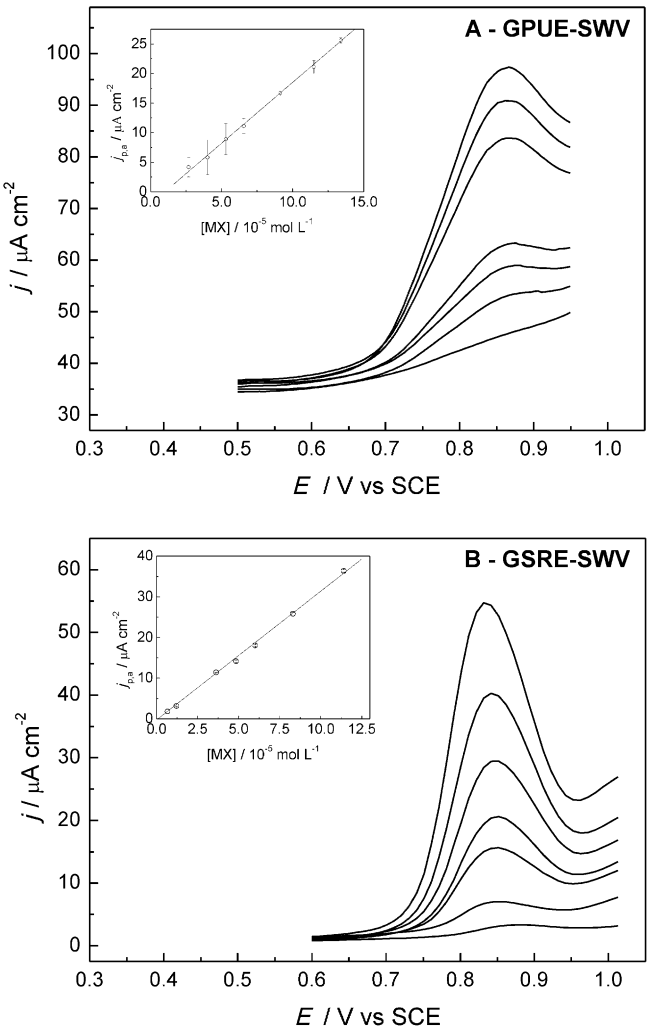

Fig. 7. Square wave voltammograms for oxidation of different concentrations of MX; the insets show analytical curves. A) GPUE, in HCl/KCl pH 2.5; [MX] = 2.68, 4.01, 5.30, 6.57, 9.12, 11.5 and 13.6×10^{-5} mol L^{-1}. SW amplitude 50 mV, potential step 5 mV, frequency 25 Hz. $E_{p,a}$ = 0.849 V vs. SCE. B) GSRE in HCl/KCl pH 2.0; [MX] = 0.666, 1.21, 3.63, 4.84, 6.00, 8.30 and 11.4×10^{-5} mol L^{-1}. SW amplitude 50 mV, potential step 10 mV, frequency 50 Hz, $E_{p,a}$ = 0.860 V vs. SCE.

1.75×10^{-5} to 1.45×10^{-4} mol L^{-1} ($j_{p,a} = 2.95\times10^{5}$ $C - 1.55$; $R = 0.9994$; $n = 7$ where C is the analytical concentration of MX in mol L^{-1}). LOD and LOQ [33] were 4.02×10^{-6} and 13.4×10^{-6} mol L^{-1}, respectively. The recoveries were between 96 to 107 %, depending on the commercial sample.

Using a GSRE (Figure 6B) in pH 2.0, a peak was observed at 0.80 V (vs. SCE). The linear range was from 0.266×10^{-5} to 2.28×10^{-5} mol L^{-1} ($j_{p,a} = 2.17\times10^{6}$ $C - 1.59$; $R = 0.9992$; $n = 5$ where C is the concentration of MX in mol L^{-1}) with LOD and LOQ of 1.35×10^{-6} and 4.50×10^{-6} mol L^{-1}, respectively [35]. Recoveries were between 93 and 100 %, depending on the sample.

Table 3 presents the values obtained during application to the commercial samples, together with the labeled and chromatographic values. The t-Student test gave agreement with the chromatographic procedure within a 90 % confidence level.

3.4.3 Square Wave Voltammetry (SWV)

The square wave parameters were optimized, first the potential increment in the interval of 5 to 10 mV and frequency from 25 to 50 Hz with pulse amplitude fixed at 50 mV. The pH values were those found to be best in the CV experiments. Figure 7 depicts the SWV profiles for both electrodes.

The best conditions using the GPUE (Figure 7A) were reached using 25 Hz, 50 mV (amplitude) and 5 mV (step potential), the oxidation peak being observed at + 0.85 V. The linear range between 2.68×10^{-5} and 13.6×10^{-5} mol L^{-1} MX. In this range the current vs. concentra-

Table 4. Summary of figures of merit obtained during MX determination at GSRE and GPUE electrodes, under the optimized conditions for CV, SWV and DPV.

Figure of merit	GPUE			GSRE		
	CV	DPV	SWV	CV	DPV	SWV
Linear range (10^{-6} mol L^{-1})	33.8–289	17.5–145	26.8–136	33.9–289	2.66–22.8	6.66–114
Sensitivity (10^5 μA mol^{-1} L cm^{-2})	0.576	2.95	2.05	0.524	21.7	2.84
LOD (10^{-6} mol L^{-1})	14.9	4.02	4.97	22.3	1.35	3.16
Recovery (%)	96–110	96–107	96–107	94–110	93–100	94–101

Table 5. Figures of merit from different procedures in the literature for MX determination by different techniques. *LDR*: linear dynamic range, *LOD*: limit of detection.

Technique	Sample	*LDR* (mol L^{-1})	*LOD* (mol L^{-1})	Ref.
Amperometry/FIA	Phosphate buffer pH 2	$1–1000\times10^{-7}$	–	[13]
DPV-Polarography	Pharmaceutical formulations in dimethylformamide	$1–50\times10^{-5}$	–	[3]
Polarography	Britton–Robinson Buffer pH 5	$2–50\times10^{-5}$	5×10^{-5}	[14]
Ion pair HPLC	Plasma	$9.6–480\times10^{-9}$	$2.4\ 10^{-9}$	[9]
Photometric titration	H_2SO_4 pH 2	–	1.0×10^{-3}	[10]
UV-Vis	Pharmaceutical formulations	$9.0–48\times10^{-6}$	–	[36]
UV-Vis	Britton–Robinson Buffer pH 5	$2.5–200\times10^{-6}$	1×10^{-6}	[14]
UV-Vis	Phosphate buffer pH 5, ethanol, propyleneglycol (1:1:3 v/v)	$2.8–153\times10^{-6}$	8.12×10^{-7}	[11]
UV-Vis/FIA	Pharmaceutical formulations	$1.0–50\times10^{-5}$	$8.92\ 10^{-6}$	[12]

tion plot obeying the linear relationship $j_{p,a}=2.05\times10^5\ C-2.06$ ($R=0.9994$, $n=7$), with *LOD* and *LOQ* of 4.97×10^{-6} and 1.66×10^{-5} mol L^{-1}, respectively. Recovery tests on the commercial samples gave recoveries from 96 to 107 %.

Using the GSRE (Figure 7B), the best conditions were reached using 50 Hz, 50 mV (amplitude) and 10 mV (potential increment), the oxidation peak being observed at +0.86 V. The linear range was from 0.664×10^{-5} to 1.14×10^{-4} mol L^{-1} ($j_{p,a}=3.16\times10^{-5}\ C-0.227$; $R=0.9981$; $n=7$; where C is the concentration of MX in mol L^{-1}) with *LOD* and *LOQ* of 3.16×10^{-6} and 10.5×10^{-6} mol L^{-1} respectively. Recovery tests resulted in recoveries from 94 to 101 %.

The concentration values obtained are given in Table 3 for commercial samples, compared with the label and the chromatographic values, again with agreement at the 90 % confidence level.

3.5 Comparison Between the Electroanalytical Procedures

The three electroanalytical techniques using the GPUE and GSRE can all be used for the determination of MX in pharmaceutical samples as well as in the artificial urine and plasma electrolyte solutions; the results agree with the HPLC procedure used as a comparative method. The analytical performance of both types of electrode is similar as shown by the figures of merit summarized in Table 4. The lowest *LOD* was observed by DPV at GSRE, probably due to the roughness of the electrode surface and/or to the presence of functional groups of the silicon rubber that could interact with the analyte. The ability of DPV in better discriminating the background from the Faraday current can also improve the *LOD*, despite the higher sensitivity of SWV [35].

Table 5 presents some figures of merit for various methods used in MX determination. Although not all authors report the *LOD* of their methods, one can find 10^{-9} mol L^{-1} in ion pair chromatography [9] and 10^{-7} in a spectrophotometric flow procedure [11], which are lower than those reported in the present work. However, the electrochemical method proposed here is simpler, less expensive and with less waste generation, not requiring any sample preparation.

4 Conclusions

Electroanalytical methods for the determination of MX in pharmaceutical samples and in artificial urine and plasma electrolyte solutions have been developed using GPUE and GSRE, with similar performance at both types of electrode. Agreement with the HPLC procedure has been demonstrated. The lowest *LOD* was observed by differential pulse voltammetry at GSRE.

Both types of composite electrodes presented a long lifetime showing no problems of adsorption of analyte or its oxidation products and, thus, no need of surface renewal between successive measurements. All the work presented here was performed with one of each type of electrode during 6 months. The electrodes were also used in high concentration salt solutions, in artificial plasma and urine electrolytes, which is a limitation for some chromatographic procedures and thus represents a significant advantage of the electroanalytical methods.

Acknowledgements

Financial support from the *Brazil/Portugal Bilateral Agreement* (CAPES/FCT 177/07), *FAPESP-Brazil* (Grant 08/03537-7), and from *CEMUC* (Research Unit 285), *FCT*, Portugal is gratefully acknowledged.

References

[1] S. S. Budavari, M. J. O'Neil, A. Smith, P. E. Heckelman, J. F. Kinneary, *The Merck Index,* 13th ed., Merck, Whitehouse Station, NJ **2001**, p. 6229.
[2] P.-C. Chiang, K. A. Foster, M. C. Whittle, Ching-Chiang Su, D. K. Pretzer, *J. Liquid Chromatogr. Relat. Technol.* **2006**, *29*, 2291.
[3] L. Amankwa, L. G. Chatten, S. Pons, *Analyst* **1983**, *108*, 1221.
[4] A. Ruiz-Medina, M. L. F. Córdova, A. Molina-Díaz, *Talanta* **1999**, *50*, 277.
[5] J. H. Han, O. S. Kwon, J. H. Chung, K. H. Cho, H. C. Eun, K. H. Kim, *J. Dermatol. Sci.* **2004**, *34*, 91.
[6] W. Z. Zhong, P. E. Sanders, M. J. Hauer, J. J. Vrbanae, *J. Chromatogr. B* **1998**, *705*, 39.
[7] W. Z. Zhong, *J. Pharm. Biomed. Anal.* **1998**, *16*, 1179.
[8] A. Zarghi, M. Jenabi, A. J. Ebrahimian, *Pharm. Acta Helv.* **1998**, *73*, 163.
[9] A. Zarghi, A. Shafaati, S. M. Foroutan, *J. Pharm. Biomed. Anal.* **2004**, *36*, 377.
[10] R. A. Sousa, F. S. Semaan, J. A. F. Baio, E. T. G. Cavalheiro, *Eclética Química* **2005**, *30*, 79.
[11] M. Bordbar, A. Yeganeh-Faal, J. Ghasemi, M. M. Ahari-Mostafavi, N. Sarlak, M. T. Baharifard, *Chem. Pap.* **2009**, *63*, 336.
[12] R. A. Sousa, F. S. Semaan, P. Cervini, E. T. G. Cavalheiro, *Anal. Lett.* **2011**, *44*, 349.
[13] V. Pfaffen, P. I. Ortiz, *Anal. Sci.* **2006**, *22*, 91.
[14] J. Arcos, B. García, A. Munguía, J. López Palacios, J. M. Kauffmann, G. J. Patriarche, *Anal. Lett.* **1991**, *24*, 357.
[15] D. E. Tallman, S. L. Petersen, *Electroanalysis* **1990**, *2*, 499.
[16] R. K. Mendes, S. Claro-Neto, E. T. G. Cavalheiro, *Talanta* **2002**, *57*, 909.
[17] F. Cespedes, E. Martinez-Fabregas, S. Alegret, *Trends Anal. Chem.* **1996**, *15*, 296.
[18] J. Trijueque, J. J. Garcia-Jareno, J. Navarro-Laboulais, A. Sanmatias, F. Vicente, *Electrochim. Acta* **1999**, *45*, 789.
[19] R. K. Mendes, P. Cervini, E. T. G. Cavalheiro, *Talanta* **2006**, *68*, 708.
[20] E. Pungor, É. Szepesváry, *Anal. Chim. Acta* **1968**, *43*, 289.
[21] A. C. Oliveira, S. X. Santos, E. T. G. Cavalheiro, *Talanta* **2008**, *74*, 1043.
[22] F. S. Semaan, E. T. G. Cavalheiro, C. M. A. Brett, *Anal. Lett.* **2009**, *42*, 1119.
[23] P. Cervini, E. T. G. Cavalheiro, *Anal. Lett.* **2008**, *41*, 1867.
[24] P. Cervini, E. T. G. Cavalheiro, *J. Braz. Chem. Soc.* **2008**, *19*, 836.
[25] P. Cervini, E. T. G. Cavalheiro, *Anal. Lett.* **2009**, *42*, 1940.
[26] F. S. Semaan, E. M. Pinto, E. T. G. Cavalheiro, C. M. A. Brett, *Electroanalysis* **2008**, *20*, 2287.
[27] S. X. dos-Santos, L. H. Mazo, E. T. G. Cavalheiro, *J. Braz. Chem. Soc.* **2008**, *19* 1600.
[28] R. A. de-Toledo, M. C. Santos, E. T. G. Cavalheiro, L. H. Mazo, *Anal. Bioanal. Chem.* **2005**, *381*, 1161.
[29] L. Liu, C. L. Qiu, Q. Chen, S. M. Zhang, *J. Alloys Compd.* **2006**, *425*, 268.
[30] N. Laube, B. Mohr, A. Hesse, *J. Cryst. Growth* **2001**, *233*, 367.
[31] C. M. A. Brett, A. M. Oliveira-Brett, *Electrochemistry: Principles, Methods and Applications*, Oxford University Press, Oxford **1993**.
[32] M. Stackelberg, M. Pilgram, V. Toome, *Z. Electrochem.* **1953**, *57*, 342.
[33] R. Pauliukaite, M. E. Ghica, O. Fatibello-Filho, C. M. A. Brett, *Electrochim. Acta* **2010**, *55*, 6239.
[34] J. C. Miller, J. N. Miller, *Statistics for Analytical Chemistry*, 3rd ed., Ellis Horwood, New York **1983**.
[35] E. T.G. Cavalheiro, A. Brajter-Toth, *J. Pharm. Biomed. Anal.* **1999**, *19*, 217.
[36] M. S. Mahrous, M. M. Abdelkhalek, Y. A. Beltagy, *Anal. Lett.* **1991**, *24*, 2017.

